Gated Recurrent Units for Lithofacies Classification Based on Seismic Inversion

Feng, Runhai

DOI
10.1007/978-3-031-52715-9_3

Publication date
2024

Document Version
Final published version

Published in
Artificial Intelligent Approaches in Petroleum Geosciences, Second Edition

Gated Recurrent Units for Lithofacies Classification Based on Seismic Inversion

Runhai Feng

Abstract As a qualitative indicator, subsurface lithofacies is an important parameter that can characterize hydrocarbon reservoirs for the degree of compartmentalization. In order to account for the geological dependency between data samples along the vertical direction, the feed-backward Recurrent Neural Networks is applied to classify the sequential lithofacies in the subsurface. Particularly, Gated Recurrent Units (GRU) is used, which can be dedicated to learning how to update or reset hidden states (in this case, lithofacies), such that the information flow through the system is regulated. Operating on the output layer, the *softmax* function is able to map the probability values over various possible lithofacies, and the associated uncertainty could be analyzed subsequently. In addition, the statistical Hidden Markov Models (HMM) is applied to benchmark the performance of GRU, in which the embedded transition matrix could enforce the conditional probability between different lithofacies. The designed GRU and HMM are applied to a synthetic model of the Book Cliffs and a real dataset from the Vienna Basin. Instead of using well logs, elastic rock properties from a non-linear inversion scheme are proposed as inputs for the classification purpose, which could help to overcome the location limitations of cored wells, and 2D sections of reservoir lithofacies are then obtained.

Keywords Recurrent Neural Networks · Rock properties · Lithofacies classification · Seismic inversion

1 Introduction

During the process of reservoir characterization, different reservoir parameters are expected to be estimated, such as lithofacies, porosity, permeability, etc. As a qualitative indicator, lithofacies is a very important reservoir parameter, which could imply the degree of reservoir compartmentalization, as well as the rock-physical behaviors

R. Feng (✉)
Department of Geoscience and Engineering, Delft University of Technology, Delft 2628CN, The Netherlands
e-mail: r.feng@tudelft.nl

C. Cranganu (ed.), *Artificial Intelligent Approaches in Petroleum Geosciences*,
https://doi.org/10.1007/978-3-031-52715-9_3

(Bosch et al. 2002; Garland et al. 2012; Zhou et al. 2016; Gan et al. 2019). In order to distinguish between different lithofacies, various methods have been developed. For example, Mukerji et al. (2001) predicted reservoir lithofacies and fluid types based on a statistical relation between rock-physical properties and seismic information. Using rock-physical models, Bosch et al. (2010) provided a quantitative description of reservoir properties in joint and simultaneous workflows.

Other than rock-physical templates being used, the non-linear relationship between rock properties and reservoir lithofacies could also be explored through advanced deep-learning methods. Qian et al. (2018) analyzed a seismic facies interpretation by deep convolutional autoencoders. Pires de Lima et al. (2019) used deep Convolutional Neural Networks (CNN) to aid the core description, which can achieve a high level of classification accuracy (~90%). Wei et al. (2019) developed a data padding strategy in CNN to characterize various rock facies.

However, these aforementioned methods can be regarded as pointwise, since every depth point that is fed into the classification system is treated as independent of each other. From a geological point of view, the intrinsic transitions of lithofacies along the vertical direction, such as the fining-upward trend in terms of grain size found in distributary channels, are missing (Feng et al. 2017). CNN uses convolutional filters to only consider the local information within the size of pre-defined filters, and thus it is more suitable for image segmentation at the pixel level (Goodfellow et al. 2016). Lithofacies are deposited according to geological rules, and the transition information in a long and short range cannot be accounted for by the convolutional filters in CNN. On the other hand, Recurrent Neural Networks (RNN) can employ the internal memory units to process series variables, and the connections between nodes form a directed graph (Goodfellow et al. 2016; Zhang et al. 2018). By means of a feedback loop, RNN allows information cycles, and both of the current state and what has learned from previous steps could be accounted for, which makes it suitable for time series analysis or tasks in the prediction of sequential variables, such as natural language processing. Imamverdiyev and Sukhostat (2019) developed effective deep-learning models for geological facies classification, in which 1D CNN, RNN, and support vector machine are compared with each other. Grana et al. (2020) proposed an RNN framework for the lithofacies classification. In this paper, the Gated Recurrent Units (GRU) (Cho et al. 2014), a gating mechanism in RNN, is applied to classify sequential lithofacies with temporal dependencies, and the data manipulation is processed at an intelligent level. Besides, Hidden Markov Models (HMM), that can implement the inherent orderings of lithofacies using a constructed transition matrix (Elfeki and Dekking 2001), is applied to benchmark the performance of the proposed deep learning method (Eidsvik et al. 2004; Lindberg and Grana 2015; Feng 2020a). In HMM, a Gaussian assumption is usually adopted to describe the relationship between rock properties and reservoir lithofacies, which might be insufficient when complex distributions exist.

The novelty of this paper is that both geological orderings and complex data distributions are considered by the designed neural system, which is expected to have a better classification performance, compared to traditional approaches. Additionally, the inverted rock properties from seismic data are proposed as the inputs, which

typically cover larger extents of target reservoir in a 2D or 3D way (Feng et al. 2018a) and can exclude the location limitation of borehole logs that are usually sparse in the field.

2 Methodology

Being able to recognize sequential patterns, RNN is a deep-learning algorithm applicable for serial data analysis, such as speech and handwriting recognitions (Goodfellow et al. 2016). It considers time and sequential information and has a temporal dimension. The outputs of RNN are not only influenced by weights applied to the inputs but also by hidden state vectors that represent the context based on prior inputs (x_t)/outputs (y_t) (Fig. 1) (Goodfellow et al. 2016; Grana et al. 2020). Therefore, RNN can maintain a class of states in memory cells, allowing it to perform jobs such as prediction of sequential data that are beyond the capability of feed-forward CNN.

Theoretically, RNN is entitled to capture long-term dependencies. However, in practice, training such network may fail because of vanishing or divergent gradients from long products of operation matrices (Goodfellow et al. 2016). To address this problem, gating mechanisms are proposed such that hidden states in the system can be updated or reset to regulate the information flow. Compared to the long short-term memory (LSTM) (Gers et al. 1999), Gated Recurrent Units (GRU) (Cho et al. 2014) has fewer parameters, as no output gate is assigned (Fig. 2) and is selected for classification task of sequential lithofacies in this study.

With gating support, GRU can be dedicated to learn how to reset or update hidden states, or when to skip irrelevant temporal information. For a given input x_t at time step t, the reset gate variable r_t and update variable u_t can control how much information of the previous state h_{t-1} will be remembered or copied, and are computed as follows:

$$r_t = \sigma(W_{xr}x_t + W_{hr}h_{t-1} + b_r) \tag{1}$$

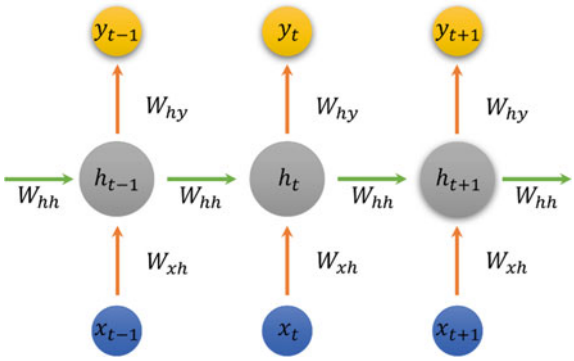

Fig. 1 Recurrent Neural Networks, with hidden state (h_t) that carries pertinent information at step t in the series. W_{xh}, W_{hh}, and W_{hy} are trainable weights associated with input (x_t)-hidden (h_t), hidden (h_{t-1})-hidden (h_t), and hidden (h_t)-output (y_t) connections, respectively

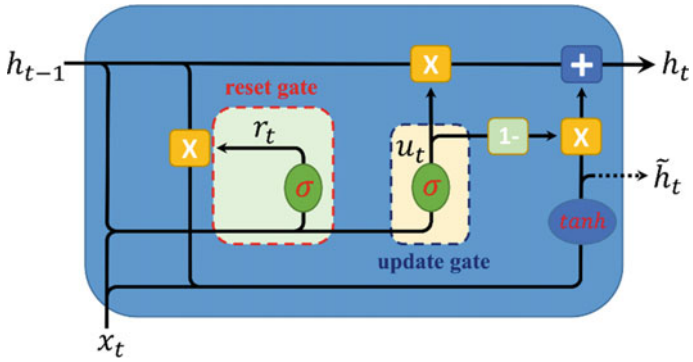

Fig. 2 Computational flow of Gated Recurrent Units

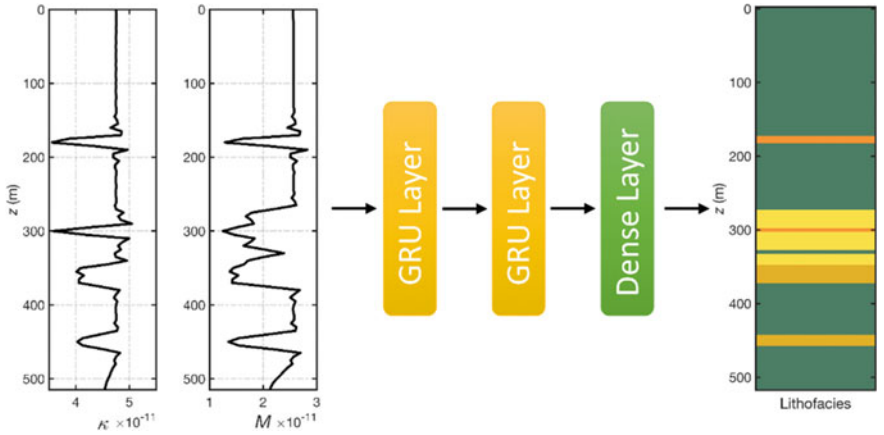

Fig. 3 Schematic view of the proposed GRU model for the lithofacies classification

$$u_t = \sigma(W_{xu}x_t + W_{hu}h_{t-1} + b_u) \tag{2}$$

where W_{xr}, W_{hr}, W_{xu}, W_{hu} and b_r, b_u are trainable weights and biases within each specific gate. σ is the *sigmoid* function with an output interval between 0 and 1.

By combining the reset gate with the effect of update gate, the new state h_t can be determined as

$$h_t = u_t \times h_{t-1} + (1 - u_t) \times \widetilde{h}_t \tag{3}$$

and

$$\widetilde{h}_t = \tanh(W_{xh}x_t + W_{hh}(r_t \times h_{t-1}) + b_h) \tag{4}$$

in which $\times$ represents an element-wise multiplication; W_{xh}, W_{hh} and b_h are trainable neural weights and biases for different states; tanh is the hyperbolic tangent activation function; and $\widetilde{h}_t$ can be considered as a candidate state, since the action of update gate has not been taken yet.

In this proposed GRU approach, the input layer is the inverted rock properties from seismic data in terms of compressibility (κ) and shear compliance (M). The network architecture includes two GRU layers with ten units for each layer. One dense layer is then added with *softmax* as the activation function, relating to the target lithofacies (Fig. 3). As a multiclass generalization/extension of the discrete Bernoulli distribution (Evans et al. 2000), *softmax* function can map the probability distributions over various possible labels after normalization (Eq. 5):

$$s_i = \frac{e^{z_i}}{\sum_{j=1}^{K} e^{z_j}} \tag{5}$$

in which, e^{z_i} is an exponential function for input vector z_i; K stands for the number of lithofacies; and s_i denotes the output probability that relates to state i (Goodfellow et al. 2016). Initial weights in these layers are randomly assigned using the Xavier initialization (Glorot and Bengio 2020), and initial biases are set to 0 before the network training. Nadam (Nesterov-accelerated Adaptive Moment Estimation) (Dozat 2016) is applied to update neural weights and biases to minimize the loss function that is a categorical cross-entropy.

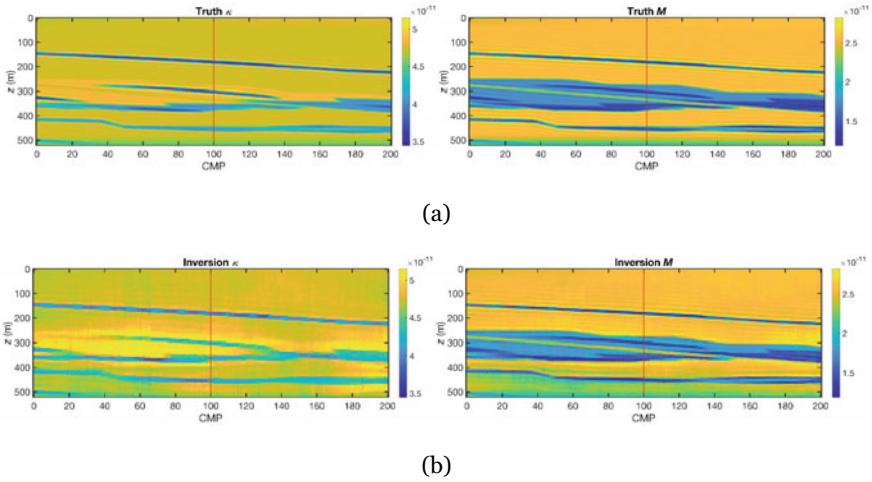

Fig. 4 True (**a**) and inverted (**b**) rock properties in terms of κ and M. The true rock properties at CMP 100 (red line in (**a**)) are used for the training of GRU system, and lithofacies are to be classified based on the input of seismic inversion results across the whole section. The unit for κ and M is square meter per newton (m^2/N)

3 Examples

3.1 Synthetic Case

The proposed methodology is first applied to a synthetic model of the Book Cliffs created by Feng et al. (2017). This geological and petrophysical model is based on the fluvio-deltaic Book Cliffs outcrops in Utah, USA, and has been added with more details by Feng et al. (2017) to emphasize the potential reservoir units. Elastic rock properties have been assigned within each lithofacies, which are generated using empirical rock equations based on different reservoir parameters, such as porosity and clay content (Feng et al. 2017). As a test, only a subset of the original 2D section has been selected, and Fig. 4 shows the true and inverted rock properties in terms of compressibility κ ($\kappa = 1/K$, with K being the bulk modulus) (Eq. 6), and shear compliance M ($M = 1/\mu$, with μ being the shear modulus) (Eq. 7):

$$\kappa = \frac{3}{3V_P^2\rho - 4V_S^2\rho} \tag{6}$$

$$M = \frac{1}{V_S^2\rho} \tag{7}$$

in which, V_P, V_S are the P- and S-wave velocities, respectively; ρ is the bulk density. κ and M are considered to be more closely related to different rock types, such that the sandstone has a large κ and a small M, since it is more easily to be compressed because of the higher porosity often found. In contrast, the shale could have a small κ and a large M, due to its weak rigidity. Moreover, κ and M can also indicate property changes in the time-lapse seismic inversion owing to their complementary property behaviors (Feng et al. 2017).

The seismic inversion approach used is a full-waveform scheme that is capable to fully explore the non-linear relationship between rock properties and seismic data (Feng et al. 2017). Compared to the truth (Fig. 4a), property values and geometrical structures in the inverted results (Fig. 4b) have been recovered quite well, which makes them as suitable inputs for lithofacies classification. For more details on the non-linear inversion scheme, please refer to Gisolf and Verschuur (2010) and Feng (2020b).

True rock properties at CMP 100 (Fig. 4a) are used to train the GRU network (Fig. 3). In total, there are four lithofacies identified at this well: Fine-grained sandstone (FS), Very fine-grained sandstone (VFS), Siltstone (SS), and Clay (Fig. 5a). Figure 5b shows the 90% confidence region of the Gaussian likelihood model in terms of κ and M, given each lithofacies. It can be seen that there is a large overlap between SS and VFS, and Clay could be easily separated from other lithofacies.

After training of the pre-designed GRU system shown in Fig. 3, the inversion results at CMP 100 (red lines in Fig. 4b) are used for the lithofacies classification (Fig. 6). Both inverted κ and M match the truth quite well, especially for M (Fig. 6a),

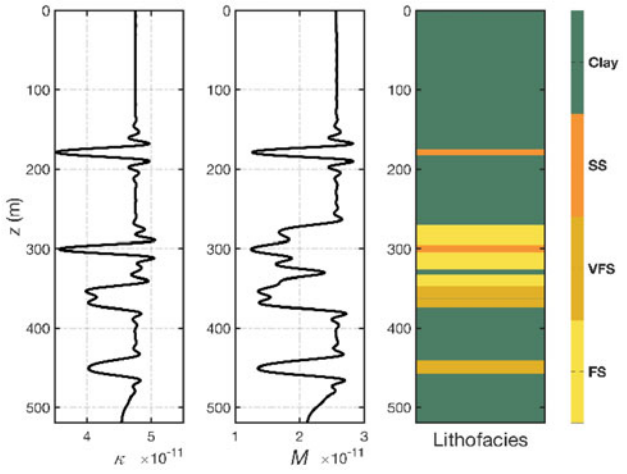

(a)

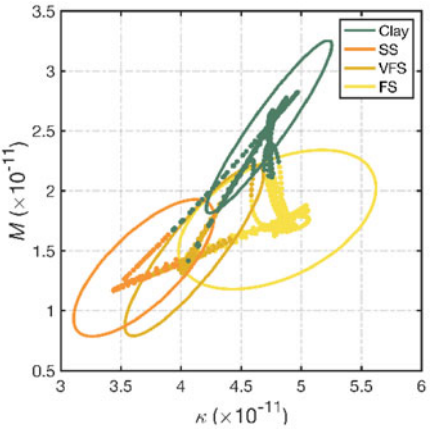

(b)

Fig. 5 **a** True rock properties and lithofacies at CMP 100 (red line in Fig. 4a) for training GRU. **b** 90% confidence region of bivariate Gaussian likelihood model given each lithofacies. Scattered points are the sample data, as colored by each lithofacies

since the PP (pressure-to-pressure) and PS (pressure-to-shear) seismic data have been used for the inversion. Compared to the reference, almost all lithofacies layers have been correctly classified by GRU, especially for the SS layer at 180 m (Fig. 6b). However, VFS is misclassified as SS between 355 and 370 m, due to the large overlap of their rock properties (Fig. 5b). The probabilities of each classified lithofacies calculated by the *softmax* function are also shown to assess the associated uncertainty,

and most of the values are close to the bounds of probability interval, 0 or 1. Notice that the true rock properties and reference lithofacies profile in Fig. 6 are obtained after upscaling of the ones in Fig. 5a to match the seismic resolution.

With the section inversion results as inputs (Fig. 4b), the classified lithofacies by GRU are shown in Fig. 7b, together with the reference (Fig. 7a). Almost all of the lithofacies units have been correctly predicted, and they are close to the truth, with some misclassified SS in the lower part.

To analyze the classification uncertainty, probabilities of each lithofacies are displayed in Fig. 8, in which the variability is less fluctuated, since these values are either close to 0 (not likely) or 1 (likely).

For a comparison with GRU, the statistical HMM is used to classify lithofacies, in which the Viterbi path is utilized, and only a single highest probability value is computed (Rabiner 1989). The transition matrix in HMM that can describe the lithofacies successions is estimated from cored wells (Fig. 5a), and the emission function for the relationship between rock properties and reservoir lithofacies is Gaussian assumed (Fig. 5b). The classified lithofacies by HMM are shown in Fig. 9.

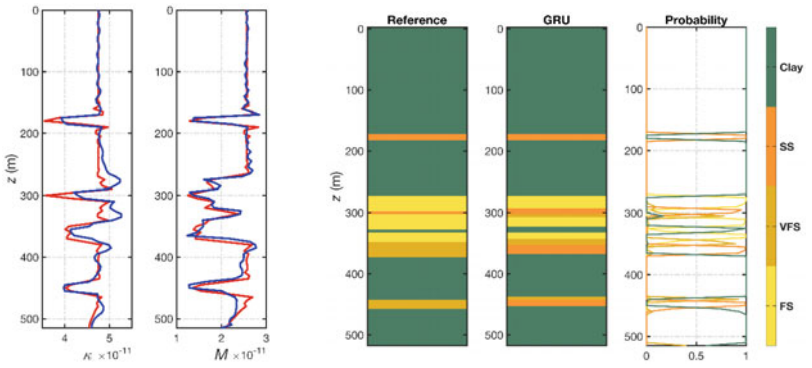

Fig. 6 **a** Inverted (blue curve) and true (red curve) rock properties at the well of CMP 100 (red lines in Fig. 4). **b** Classified lithofacies by GRU and their associated uncertainty

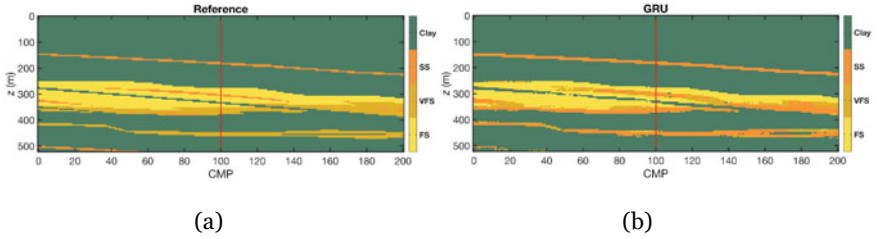

Fig. 7 Reference lithofacies (**a**) and classified results by GRU (**b**) of the whole cross section. The red line shows the CMP location for an inspection in Fig. 6b

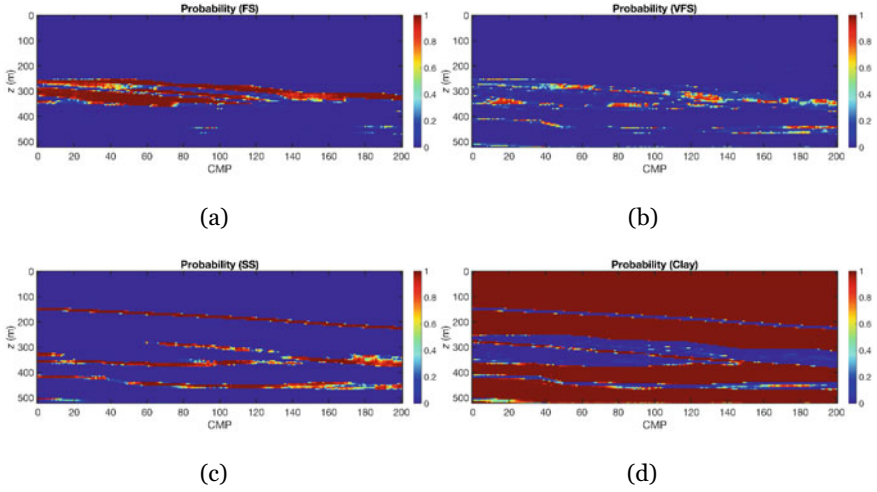

Fig. 8 Probability values of FS (**a**), VFS (**b**), SS (**c**), and Clay (**d**)

At the well location (CMP 100), compared to the results by GRU (Fig. 6b), the thin SS layer has also been predicted correctly around 180 m. Between 270 and 360 m, the result in HMM is more uniform, and Clay has been misclassified as FS between 460 and 520 m. To quantitatively analyze the categorical results by GRU and HMM at the well location, Matthews correlation coefficient (MCC) is computed, which is based on a multiclass confusion matrix, and its value range is between -1 (worst outcome) and 1 (perfect prediction) (Matthews 1975; Feng et al. 2018b). The MCC value is 0.7007 for GRU (Fig. 6b) and 0.6868 for HMM (Fig. 9a), which means that a higher accuracy by GRU has been achieved.

In the section result, the lateral continuity of SS layer around 180 m cannot be fully recovered by HMM, and there are some discontinuous VFS units being predicted (Fig. 9b). FS has been over-predicted by HMM, and the thin Clay layer in between FS is not classified around 300 m in depth (between CMP 0 and 140) (Figs. 7a and 9b). This might be caused by the large overlap between their distributions (Fig. 5b), and they cannot be fully explained by the Gaussian assumption used in HMM.

3.2 Field Case

In order to further test the capability of the proposed GRU, a field dataset from the Vienna Basin for the exploration of clastic reservoirs is used. As an extensional basin between the Eastern Alps and the Western Carpathians, a major part of the basin fills are shallow water sediments of marine to limnic, and fluviatile origins deposited in the Early to Middle Miocene age (Strauss et al. 2006). The main reservoirs in this basin are from Sarmatian and Badenian times (Strauss et al. 2006). Vintages of 3D

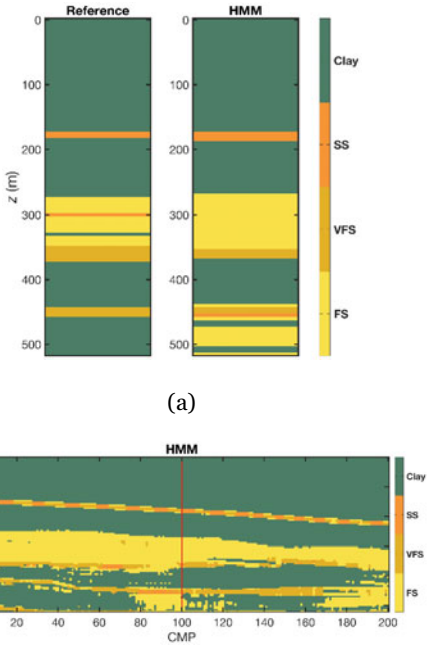

Fig. 9 Classified lithofacies by HMM at the well location (CMP 100) (**a**) and of the cross section (**b**). The red line shows the well location for training

seismic surveys acquired in different years have been merged into a single dataset, namely Vienna Basin Super Merge (VBSM). These pre-stack seismic gathers are used as inputs for the non-linear inversion scheme (Feng et al. 2017, 2018a), and a single cross section of inverted κ and M is shown in Fig. 10, where there is a logging well drilled in the middle (CMP 70).

Figure 11a shows the rock properties and interpreted lithofacies at the well location (CMP 70) (Shale, Shaly Sand (SH_Sand), and Sand). Lithofacies are identified by petrophysicists based on different contents of clay minerals, as more clay minerals are found from the shale, while less clay minerals are contained in the sand. It can

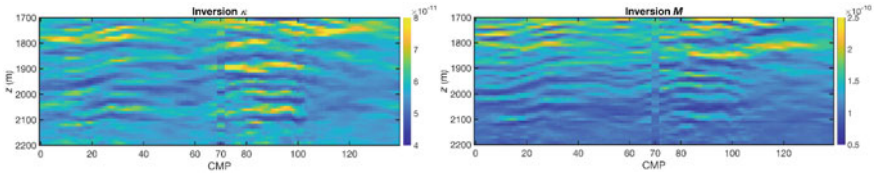

Fig. 10 Cross section of inverted rock properties in the Vienna Basin. **a** κ; **b** M. The logging properties at CMP 70 have been superposed on the inversions for a comparison

be seen from the confidence region and sample data in Fig. 11b that there are large overlaps between the three lithofacies, which would make the distinguish between them difficult.

Figure 12 displays the true and inverted rock properties at the well location (CMP 70). The quality of the inverted results is suboptimal, even though the match in the upper part is quite good. The lower part in the inversion matches the truth worse, which is attributed to the poorer seismic-to-well tie with an increase in depth. The inversion quality of M is worse than that of κ, since only PP data are available in the field.

After training based on the well-log data at CMP 70, the classified lithofacies with seismic inversions as inputs by HMM and GRU are shown in Fig. 13, in which the probability of each lithofacies is calculated by the *softmax* function in GRU. Both methods could recover the main Sand reservoir units in the upper part, while HMM predicts more Sand than GRU in the lower part. All the Shale layers have been overestimated by HMM and GRU. The MCC value is 0.1714 by GRU, which is higher than 0.0544 by HMM.

The confusion matrices showing the success and failure rates by classifiers for each lithofacies are displayed in Fig. 14. The correctly classified data samples and

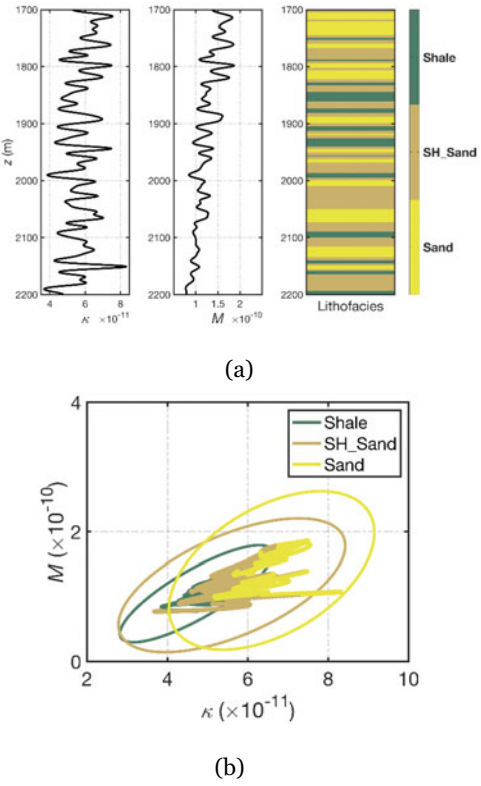

Fig. 11 **a** Rock properties and interpreted lithofacies at the well location (CMP 70). **b** 90% confidence region of bivariate Gaussian likelihood function given each lithofacies. Colored points are the sample data

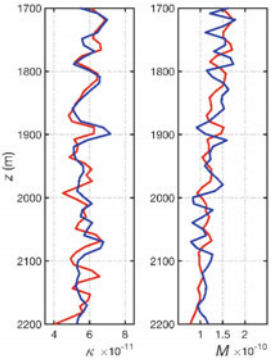

Fig. 12 True (red curve) and inverted (blue curve) rock properties at the well location (CMP 70). An upscaling is performed for rock properties shown in Fig. 11a to match the seismic scale

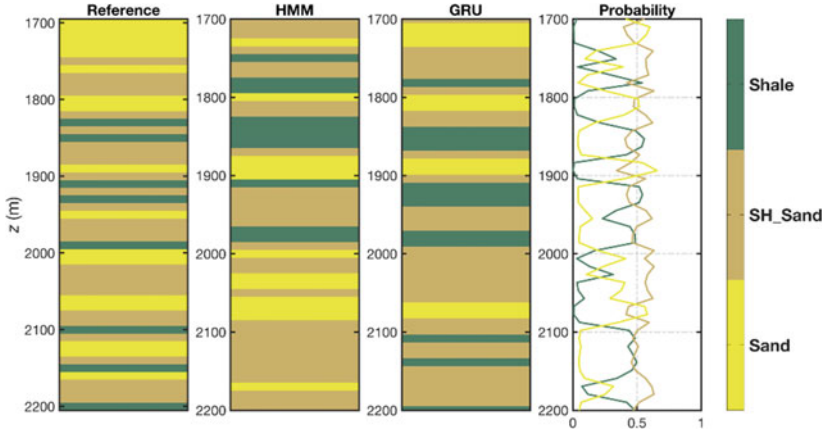

Fig. 13 Classified lithofacies by HMM and GRU at the well location (CMP 70). The reference profile is obtained by upscaling the true lithofacies at the well (Fig. 11a) to the seismic resolution

their related percentages are shown along the diagonal space, in which a score of 100% means a perfect classification. A suboptimal classification is obtained, if the classified samples are close to the diagonal, such that Sand is predicted as SH_Sand. The worst classification samples are those in the off-diagonal space, since the reservoir Sand has been misclassified as non-reservoir Shale or vice versa. GRU performs better than HMM for the classification of Sand and SH_Sand. For the classification of Shale, the same performance can be observed between them within the diagonal samples.

Based on the non-linear inverted rock properties of the cross-sectional seismic data (Fig. 10), the classified lithofacies by GRU are shown in Fig. 15, together with their corresponding probabilities. Most data samples have been classified as SH_Sand, which is also indicated by the reference lithofacies at the well location (Figs. 11a

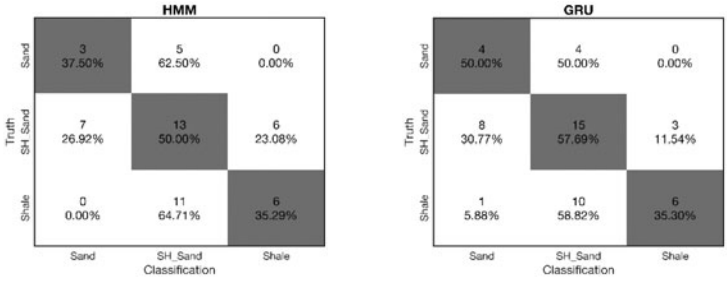

(a) (b)

Fig. 14 Confusion matrices of HMM (**a**) and GRU (**b**), in which the gray color is associated with the diagonal cells where the classification is correct

and 13). Small Sand reservoir units are distributed across the section, separated by the Shale layers, which are conformable with the depositional environments of shallow marine and limnic origins with sand sheets and impermeable shales in between the Vienna Basin (Strauss et al. 2006).

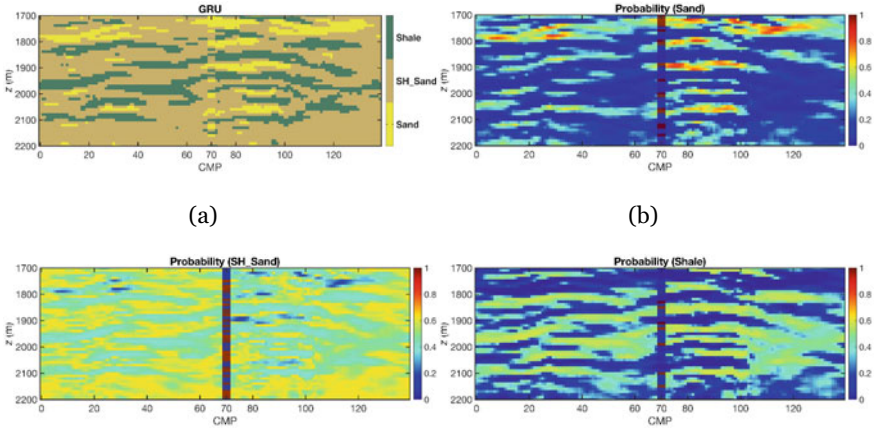

(a) (b)

(c) (d)

Fig. 15 **a** Classified lithofacies by GRU with inverted rock properties of the cross section as inputs (Fig. 10). Probability as calculated by *softmax* function in GRU for Sand (**b**), SH_Sand (**c**), and Shale (**d**). The reference lithofacies and their probability values (0 or 1) at the well location (CMP 70) are superposed on the sections

4 Discussion

In this paper, instead of using well logs, which have location limitations, the inversion results from seismic data are proposed as inputs for the classification purpose and a 2D section of reservoir lithofacies is obtained. The non-linear inversion scheme used in this paper is based on an integral representation of the full-elastic equations (Gisolf and Verschuur 2010), in which all internal transmission effects and internal multiples are considered, as well as the wave-mode conversions. The number of iterations will determine the order of multiples used in the inversion procedure. A good recovery of subsurface properties and geometries could be guaranteed (Gisolf and Berg 2010a, 2010b), which makes the inversion results as good candidate inputs for the lithofacies classification. The inverted κ (compressibility) and M (shear compliance) are deemed to relate more closely to lithofacies types (Feng et al. 2018a).

In the synthetic study, both PP and PS seismic data are used as inputs for the non-linear inversion scheme, which makes that the quality of κ and M are almost equally good (Figs. 4 and 6a). When only PP data are available such as in the field example, κ is determined better than M (Fig. 12). Another rock property—bulk density has strong connections with lithofacies and is only accessible when high-quality and wide-angle seismic gathers are available.

A comparison is made between GRU and HMM for the lithofacies classification since both methods could account for the data dependency along the vertical direction. In HMM, there is a Gaussian assumption used to draw the relationship between rock properties and reservoir lithofacies (Figs. 5b and 11b), which is not able to explain complex data distributions. Differently, the non-parametric GRU could relax the strong assumption of Gaussianity in HMM by fitting the non-linear relations between rock properties and reservoir lithofacies with the aid of synaptic neurons. Compared to the results by HMM, GRU can achieve a higher classification accuracy (larger MCC values), especially in the synthetic study for its ability to predict the SS layer around 180 m across the whole section (Fig. 7b).

To train the GRU system, logging data at the well location are used (CMP 100 in Fig. 5a and CMP 70 in Fig. 11a), and the seismic inversion results have been kept untouched during the training process, which can be considered as a blind test set. The training of GRU for 5000 epochs took ~2 min and ~6 min for synthetic and real studies, respectively, on a Xeon 3.70 GHz CPU (central processing unit). Afterward, the implementation of trained GRU on the remaining trace locations is very fast, which can greatly improve the computational efficiency, especially when a large volume of seismic inversion results is available, compared to other traditional rock physics-based methods.

Softmax function is applied to calculate the probability values of lithofacies, given the input rock properties. In the synthetic study, in total, there are 1300 data samples, which may not be representative enough for data distributions, especially for SS. Thus, the so-obtained probability values are less varied (Figs. 6b and 8), compared to the ones in the real case study (Figs. 13 and 15b–d). In the field example, there are 3417 data samples at the selected well location for the GRU training. It is important

to note that the same training data in GRU are used for the estimation of parameters in HMM.

Design of network architecture and hyper-parameters tuning are important steps for a successful retrieval of reservoir lithofacies. A trial-and-error approach is usually adopted to select the hyper-parameters in GRU system for the classification task. In this research, a simple network architecture is used that can already provide a high accuracy, especially in the synthetic study. Other complex network structures could also be applied, which are still under investigation. To prevent the overfitting problem, a regularization technique combining batch-normalization and dropout is employed (Srivastava et al. 2014; Ioffe and Szegedy 2015). Moreover, since the proposed neural model is supervised, which means that a perfect classification performance can only be expected when lots of labelled examples are available, and the rock-physical features given lithofacies should be well-defined such that the intra-state variance is as low as possible, and the extra-state variance is wide enough.

As a regression process, reservoir porosity is to be predicted in the future, which could help to quantify the storage potential of hydrocarbon reservoirs. Furthermore, the implemented GRU system could be modified in order to account for the horizontal correlation between lithofacies (Feng et al. 2018a; Tan et al. 2019), which is missed in this study, since the current classification process is implemented trace-by-trace.

5 Conclusion

Gated Recurrent Units (GRU), a special form of Recurrent Neural Networks, was applied for the lithofacies classification, which is a qualitative indicator for hydrocarbon reservoirs. The designed GRU network could account for the spatial coupling between data points along the vertical direction. Therefore, the classification process could implicitly honor the geologically depositional rules. Meanwhile, the data manipulation has been taken to an intelligent level, instead of common Gaussian assumption being adopted, such as in Hidden Markov Models. Rather than using well-log data, which are only available at sparse locations in the field, results from a non-linear inversion scheme on seismic data are used as inputs in the classification process, and 2D sections are produced.

Acknowledgements This study is sponsored by the DELPHI Consortium. OMV is gratefully acknowledged for permission to publish this data.

Declaration of Interests The authors declare that they have no known competing financial interests or personal relationships that could have appeared to influence the work reported in this paper.

References

Bosch M, Zamora M, Utama W (2002) Lithology discrimination from physical rock properties. Geophysics 67(2):P573–P581

Bosch M, Mukerji T, Gonzalez EF (2010) Seismic inversion XE "Seismic inversion" for reservoir properties combining statistical rock physics and geostatistics: a review. Geophysics 75(5):A165–A176

Cho K, Merrienboer B, Gulcehre C et al (2014) Learning phrase representations using RNN encoder-decoder for statistical machine translation. arXiv:1406.1078

Dozat T (2016) Incorporating nesterov momentum into adam. ICLR workshop

Eidsvik J, Mukerji T, Switzer P (2004) Estimation of geological attributes from a well log: an application of hidden Markov chains. Math Geol 36(3):379–397

Elfeki A, Dekking M (2001) A Markov chain model for subsurface characterization: theory and applications. Math Geol 33(5):569–589

Evans M, Hastings N, Peacock B (2000) Statistical distributions. Wiley

Feng RH, Luthi SM, Gisolf A, Sharma S (2017) Obtaining a high-resolution geological and petrophysical model from the results of reservoir-orientated elastic wave-equation-based seismic inversion. Pet Geosci 23:376–385

Feng R, Luthi SM, Gisolf A, Angerer E (2018a) Reservoir lithology determination by hidden Markov random fields based on a Gaussian mixture model. IEEE Trans Geosci Remoting Sens 56(11):6663–6673

Feng R, Luthi SM, Gisolf D (2018b) Simulating reservoir lithologies by an actively conditioned Markov chain model. J Geophys Eng 15(3):800–815

Feng R (2020a) Lithofacies classification based on a hybrid system of Artificial Neural Networks and Hidden Markov Models. Geophys J Int

Feng R (2020b) Estimation of reservoir porosity based on seismic inversion results using deep learning methods. J Nat Gas Sci Eng. https://doi.org/10.1016/j.jngse.2020.103270

Gan L, Wang Y, Luo X et al (2019) A permeability prediction method based on pore structure and lithofacies. Pet Explor Dev 46(5):935–942

Garland J, Neilson J, Laubach SE, Whidden KJ (2012) Advances in carbonate exploration and reservoir analysis. Geol Soc Lond Spec Publ 370:1–15

Gers FA, Schmidhuber J, Cummins F (1999) Learning to forget: continual prediction with LSTM. In: Proceedings of the ICANN'99. IEEE, pp 850–855

Gisolf A, Van Den Berg PM (2010) Target oriented non-linear inversion of seismic data. In: 72nd annual international meeting of European association of geoscientists and engineers (expanded abstract), Barcelona, 14–17 Jun, 2010

Gisolf A, Van Den Berg PM (2010) Target-oriented non-linear inversion of time-lapse seismic data. In: 80th annual international meeting of society of exploration and geophysics (Expanded Abstract), Denver, 17–22 Oct, 2010

Gisolf A, Verschuur DJ (2010) The principles of quantitative acoustical imaging. EAGE Publications b.v., Houten

Glorot X, Bengio Y (2020) Understanding the difficulty of training deep feedforward neural networks. In: Proceedings of the 13th international conference on artificial intelligence and statistics, pp 249–256

Goodfellow I, Bengio Y, Courville A (2016) Deep learning. MIT Press

Grana D, Azevedo L, Liu M (2020) A comparison of deep machine learning and Monte Carlo methods for facies classification from seismic data. Geophysics 85(4):WA41–WA52

Imamverdiyev Y, Sukhostat L (2019) Lithological facies classification using deep convolutional neural network. J Petrol Sci Eng 174:216–228

Ioffe S, Szegedy C (2015) Batch normalization: accelerating deep network training by reducing internal covariate shift. In: Proceedings of the 32nd international conference on international conference on machine learning

Lindberg DV, Grana D (2015) Petro-elastic log-facies classification using the expectation-maximization algorithm and hidden Markov models. Math Geosci 47:719–752

Matthews BW (1975) Comparison of the predicted and observed secondary structure of T4 phage lysozyme. Biochimica et Biophysica Acta (BBA)—Protein Structure 405(2):442–451

Mukerji T, Jørstad T, Avseth P, Mavko G, Granli JR (2001) Mapping lithofacies and pore-fluid probabilities in a North Sea reservoir: seismic inversions and statistical rock physics. Geophysics 66(4):988–1001

Pires de Lima R, Suriamin F, Marfurt KJ, Pranter MJ (2019) Convolutional neural networks as aid in core lithofacies classification. Interpretation 7(3):SF27–SF40

Qian F, Yin M, Liu X, Wang Y, Lu C, Hu G (2018) Unsupervised seismic facies analysis via deep convolutional autoencoders. Geophysics 83(3):A39–A43

Rabiner LR (1989) A tutorial on hidden Markov models and selected applications in speech recognition. Proc IEEE 77(2):257–286

Srivastava N, Hinton G, Krizhevsky A et al (2014) Dropout: a simple way to prevent neural networks from over-fitting. J Mach Learn Res 15:1929–1958

Strauss P, Harzhauser M, Hinsch R, Wagreich M (2006) Sequence stratigraphy in a classic pull-apart basin (Neogene, Vienna Basin). A 3D seismic based integrated approach. Geol Carpathica 57(3):185–197

Tan X, Liu Y, Zhou X (2019) Multi-parameter quantitative assessment of 3D geological models for complex fault-block oil reservoirs. Pet Explor Dev 46(1):194–204

Wei Z, Hu H, Zhou H, Lau A (2019) Characterizing rock facies using machine learning XE "Machine learning" algorithm based on a Convolutional Neural Network and data padding strategy. Pure Appl Geophys 176:3593–3605

Zhang D, Chen Y, Meng J (2018) Synthetic well logs generation via recurrent neural networks. Pet Explor Dev 45(4):629–639

Zhou Z, Wang G, Ran Y et al (2016) A logging identification method of tight oil reservoir lithology and lithofacies: a case from Chang7 Member of Triassic Yanchang Formation in Heshui area. Ordos Basin NW China Pet Explor Dev 43(1):65–73